MOLECULAR AND CELLULAR BIOLOGY, Nov. 1996, p. 6252–6262 Vol. 16, No. 11
0270-7306/96/$04.00+0

Clonal Analysis of Delayed Karyotypic Abnormalities and Gene Mutations in Radiation-Induced Genetic Instability

ANDREW J. GROSOVSKY,[1,2]* KARYN K. PARKS,[2] CYNTHIA R. GIVER,[2] AND STEPHEN L. NELSON[1]

Biomedical Sciences[1] and Environmental Toxicology[2] Graduate Programs, University of California, Riverside, California

Received 5 June 1996/Returned for modification 19 July 1996/Accepted 8 August 1996

Many tumors exhibit extensive chromosomal instability, but karyotypic alterations will be significant in carcinogenesis only by influencing specific oncogenes or tumor suppressor loci within the affected chromosomal segments. In this investigation, the specificity of chromosomal rearrangements attributable to radiation-induced genomic instability is detailed, and a qualitative and quantitative correspondence with mutagenesis is demonstrated. Chromosomal abnormalities preferentially occurred near the site of prior rearrangements, resulting in complex abnormalities, or near the centromere, resulting in deletion or translocation of the entire chromosome arm, but no case of an interstitial chromosomal deletion was observed. Evidence for chromosomal instability in the progeny of irradiated cells also included clonal karyotypic heterogeneity. The persistence of instability was demonstrated for at least 80 generations by elevated mutation rates at the heterozygous, autosomal marker locus *tk*. Among those TK^- mutants that showed a loss of heterozygosity, a statistically significant increase in mutation rate was observed only for those in which the loss of heterozygosity encompasses the telomeric region. This mutational specificity corresponds with the prevalence of terminal deletions, additions, and translocations, and the absence of interstitial deletions, in karyotypic analysis. Surprisingly, the elevated rate of TK^- mutations is also partially attributable to intragenic base substitutions and small deletions, and DNA sequence analysis of some of these mutations is presented. Complex chromosomal abnormalities appear to be the most significant indicators of a high rate of persistent genetic instability which correlates with increased rates of both intragenic and chromosomal-scale mutations at *tk*.

Carcinogenesis is a multistep process involving mutations in multiple tumor suppressor genes and oncogenes which lead to an increasingly malignant phenotype (8, 53, 60). Mutations in tumor cells include chromosomal aberrations such as deletions, loss of heterozygosity (LOH), translocations, amplifications, and aneuploidy, as well as intragenic DNA sequence alterations such as base substitutions and frameshifts. It has been suggested that the large number of mutations in tumor cells cannot be accounted for by spontaneous processes and that a mutator phenotype may be involved (40). Karyotypic heterogeneity is a hallmark of tumor cells, and it is well documented that tumor cells undergo a variety of chromosomal changes during malignant progression (28, 35, 48). Data demonstrating similar increases in point mutations are more limited and inconsistent. Hereditary nonpolyposis colon cancer, an inherited cancer syndrome due to germ line mutations in mismatch repair genes (45), is characterized by microsatellite instability (54) and increased point mutation rates (3, 10). On the other hand, studies of other tumor types have not consistently found an increase in intragenic mutation rates (2, 9, 13, 24, 57, 61).

Several lines of evidence indicate that ionizing radiation can induce persistent genetic instability in a high proportion of exposed cells. Carcinogenesis studies performed both in vitro and in vivo have shown that a large fraction of exposed cells undergo initiation (31, 32). These results indicate the existence of a high-frequency and persistent cellular response activated by carcinogen exposure, rather than a mutation in a specific cellular gene. This cellular process enhances the probability of a subsequent mutational step, leading to the malignant transformation of one or more of the progeny of the irradiated cells (23, 31, 32, 47). One well-documented manifestation of genetic instability has been elevated rates of nonclonal karyotypic abnormalities, occurring at a delayed time after exposure to ionizing radiation, in the progeny of irradiated cells. X-irradiation was demonstrated to induce delayed chromosomal instability in a human-hamster hybrid cell line (41) and to induce clonal karyotypic heterogeneity in human T lymphocytes (20, 21). Densely ionizing radiation such as α particles (25–27) and heavy ions (42, 56) have been shown to induce chromosomal instability in mouse and human bone marrow cells and fibroblasts. Studies of delayed mutations have been much more limited; one study (6) reported a persistent, radiation-induced elevation in mutation frequency at the hemizygous hypoxanthine phosphoribosyltransferase locus (*hprt*) in CHO cells. In a seemingly related phenomenon, a persistent reduction in cloning efficiency for the progeny of the irradiated cells, referred to as delayed reproductive death, has been observed (5, 33, 49). These studies suggest that radiation exposure induces a persistent destabilization of the genome, leading to the delayed expression of lethal mutations (5, 33, 49).

It has been postulated that chromosomal instability plays a significant role in tumor progression (8, 40, 53). Presumably, chromosomal alterations may contribute to malignant progression by associated aneuploidy or gene amplification or by generating multilocus mutation events which involve many genes, including specific oncogenes or tumor suppressor loci within the affected chromosomal region. This model predicts that the rate of intragenic mutations would not be directly affected by chromosomal level instability but that mutants attributable to a LOH, reflecting large-scale deletion or recombinational events, would be significantly elevated. In one study, elevated rates of large-scale deletions have been reported at the auto-

* Corresponding author. Mailing address: University of California, Environmental Toxicology, 5419 Boyce Hall, Riverside, CA 92521. Phone: (909) 787-3193. Fax: (909) 787-3087. Electronic mail address: Grosovsk@mail.ucr.edu.

somal locus *aprt* in a tumor cell line, although no parallel analysis of chromosomal instability was performed (19). Other investigations of this type have been restricted to the use of marker loci which either are hemizygous or require an intragenic base substitution for selection of a viable mutant, and no consistent elevation of specific locus mutation rate has been reported (2, 3, 9, 10, 13, 24, 57, 61). Mechanisms for the expression of recessive mutations at heterozygous, autosomal loci include intragenic mutation of the dominant, wild-type allele; gene conversion; or a variety of extra-allelic events resulting in homozygosity or hemizygosity of the target locus (4). Most of these mechanisms of mutagenesis are not available in hemizygous situations. Large multilocus deletions, for example, may not be recoverable as viable mutants of a hemizygous gene since they may include essential genes which happen to be within the region of hemizygosity (18, 51). Because of the heterozygous nature of the selectable autosomal marker locus for thymidine kinase (*tk*) in TK6 human lymphoblasts, we are able to measure both point mutations and LOH events to determine whether either or both are elevated in cells demonstrating radiation-induced chromosomal instability.

In a previous investigation, spontaneous and radiation-induced HPRT$^-$ total-gene deletions were collected and mapped by using linked sequence-tagged-site (STS) markers (51). Several of the X-ray-induced deletions were shown to be greater than 3 Mb in length. The present study originated simply as a determination of whether these large, radiation-induced deletions affecting the *hprt* locus could be visualized cytogenetically by G-banding analysis of metaphase chromosomes. Although none of the deletions at *hprt* were associated with a cytogenetically visible alteration affecting Xq26, it was observed that many of the X-ray-induced HPRT$^-$ mutants exhibited other karyotypic abnormalities and heterogeneity. These initial observations led to a more systematic analysis involving additional experimental groups which demonstrated clonal karyotypic heterogeneity, and complex chromosomal rearrangements, in a high percentage of irradiated TK6 lymphoblasts. We then used *tk* as a marker locus to demonstrate that mutation rates are persistently and significantly elevated in clones exhibiting chromosomal instability manifested as complex rearrangements. Analysis of delayed TK$^-$ mutants demonstrated that the mutator effect is partially attributable to chromosomal-scale LOH corresponding to the delayed cytogenetic abnormalities. Surprisingly, a significant increase in intragenic point mutation rate also contributed to the overall mutator effect.

MATERIALS AND METHODS

Cell line, marker loci, and radiation sources. TK6 is a human B-lymphoblastoid cell line (38) which is maintained in exponentially growing suspension cultures at concentrations up to 10^6 cells per ml. The *hprt* locus is located at Xq26, and the *tk* locus has been mapped to chromosome 17q23-25 (11). The *tk* gene is 12.9 kb long, with seven exons comprising 702 bp of coding sequence (12). Two polymorphic single-base-insertion frameshifts were found within the coding region of the *tk* locus in TK6 cells (16). An inactivating frameshift was identified within exon 4 of the nonfunctional allele, and a second, phenotypically silent frameshift is located in exon 7 of the functional allele.

For the collection of radiation-induced HPRT$^-$ mutants, irradiation was performed in complete medium with 80-keV constant-potential X rays delivered at a dose rate of 24 cGy/min (50). Because of a change in source availability, subsequent collections of irradiated clones were made with a cesium-137 gamma source (J. L. Shepherd and Associates) at a dose rate of 10.1 cGy/min, as previously described (52).

Collection and origin of clones used for analysis of genetic instability. Collection and molecular analyses of the spontaneous and radiation-induced HPRT$^-$ mutants were previously reported (15, 50, 51), and procedures for collection of independent spontaneous or induced mutants have been published elsewhere (38). All of the spontaneous and radiation-induced HPRT$^-$ mutants examined were total-gene deletions, including some greater than 3 Mb in length (51). Briefly, mutants were collected by a modified fluctuation analysis protocol. Cultures were started from small initial inocula (10^3 cells) and expanded to 20-ml cultures at approximately 10^6 cells per ml. Immediately following 200-cGy X-irradiation, 20 ml of fresh medium was added to each culture, and subculture was performed as required during a 7-day phenotypic expression period prior to selection of mutants. Irradiation with 200 cGy reduced the mean surviving fraction to 0.06 (50). Clonal selection of HPRT$^-$ mutants was performed in 96-well dishes (4×10^4 cells per well) in RPMI 1640 containing 10% iron-supplemented calf serum (HyClone), and 5 μg of 6-thioguanine (6-TG) per ml. The average cloning efficiency of TK6 cells was approximately 0.60. Spontaneous mutants were collected either from cultures established in parallel with those to be exposed or in separate experiments. Only one mutant was recovered from each independent culture in order to preclude the collection of sibling clones. Mutants were picked after 2 weeks of growth for colony formation in 96-well dishes and then expanded for an additional 2 weeks in T flasks, at which point several aliquots of approximately 3×10^6 cells were frozen for storage. Two other groups of clones were also collected; one group was exposed to 200-cGy γ-irradiation but not selected in 6-TG, and the second group was unirradiated and not selected in 6-TG. These clones were collected by establishing independent cultures from small initial inocula as above, although no expression period was required. Only one clone was collected from each independent culture, as in the case of mutant collections. Seeding density in 96-well dishes was 2 cells per well for unirradiated cells and adjusted according to the surviving fraction (0.06 [50]) to 20 cells per well for 200-cGy-irradiated cells.

Cytogenetic analysis. Cultures were grown to a density of 10^6 cells per ml in 15 ml for metaphase harvesting. Metaphase preparation was performed according to standard procedures, as briefly outlined here. Ethidium bromide (150 μl of a 0.05% solution) was added to each culture for a 30-min incubation at 37°C; this was followed by addition of 75 μl of Colcemid (10 μg/ml; Gibco BRL) and incubation at 37°C for 2.5 h. The contents of the flasks were then centrifuged for 10 min at $188 \times g$ and resuspended in 10 ml of KCl (0.56%; Sigma) prewarmed to 37°C. Following incubation at 37°C in the hypotonic solution for approximately 16 min, 1 ml of −20°C Carnoy's fixative (3:1 methanol-acetic acid; Fisher Scientific) was added to each culture to stop further cell swelling. The cells were then centrifuged and resuspended in −20°C Carnoy's fixative four times, dropped onto clean slides, and aged for 3 days at 60°C on a slide warmer (Fisher). Slides were then banded for 18 s with 0.2× trypsin in phosphate-buffered saline (Irvine Scientific), rinsed twice in 1× Gurr's buffer (Bio/medical Specialties), and stained for 3 min with Giemsa stain (Harleco; 3 ml of a solution of 7.4 g of Giemsa stain per liter of methyl alcohol diluted in 47 ml of Gurr's buffer). Slides were examined with an Olympus model BH-2 light microscope. Ten to twenty metaphases were examined for each of 68 independent clones.

Mutation rate determinations at the *tk* locus. Mutation rates were determined by inoculating 16 flasks with 10^3 cells and then allowing expansion to approximately 10^7 cells per culture. Once the final cell number was reached, the entire culture was plated in 96-well dishes (4×10^4 cells per well) for selection of TK$^-$ mutants in medium containing 2 μg of trifluorothymidine per ml (14). After 11 days of growth, the mutation rates of normal-growth TK$^-$ mutants (34, 39, 68) were calculated by the P_o method (37). The plates were refed with trifluorothymidine and incubated for an additional 7 days to determine the mutation rates of slowly growing TK$^-$ mutants (34, 39, 68). In some cases, the mutation rate for slow-growth TK$^-$ mutants was so elevated that all of the 16 flasks used for the determination of mutation rate contained at least some mutant clones. A minimal mutation rate was estimated by assuming that one flask in each group was devoid of mutants.

LOH analysis of TK$^-$ mutants. We utilized a rapid LOH screen for TK$^-$ normal-growth mutants using PCR amplification and single-nucleotide DNA sequencing at an exon 7 frameshift polymorphism site distinguishing the parental alleles. This assay is designed to rapidly partition TK$^-$ mutations into two categories: exon 7 heterozygotes, which include all point mutants, and homozygotes, which include all LOH mutants (14). As previously described (14), a 1,016-bp fragment carrying *tk* exons 5 to 7 was PCR product amplified and then column purified (QIAquick-spin PCR Purification Kit; Qiagen). Thermocycle DNA sequencing (*fmol* system; Promega) was performed for the exon 7 region containing the frameshift polymorphism in every TK$^-$ mutant by using a single dideoxynucleotide reaction (14). TK$^-$ mutants which remain heterozygous exhibit a characteristic double-banded pattern when sequencing through and beyond the frameshift regions.

TK$^-$ mutant cDNA sequencing and Southern blotting. RNA preparation, reverse transcription-PCR, and PCR amplification and sequencing of *tk* cDNA were performed as described previously (14, 16). PCR amplification and sequencing of genomic fragments for sequencing were done as required (14, 16). Southern blotting was performed using the Genius system (Boehringer Mannheim) and a PCR-amplified *tk* cDNA probe as previously reported (14).

Statistical methods. Significance levels were determined by using the software package Instat (GraphPad, San Diego, Calif.). Statistical analysis of differences in mutation rates was performed using a two-tailed unpaired *t* test. Comparison of mutational spectra used contingency tables (2 by 2) with mutually exclusive cells and Fisher's exact test as previously reported (50).

TABLE 1. Clonal karyotypic analysis of genetic instability

Mutant(s) or clone(s)	Karyotype[a,b,c]	Fraction of metaphases examined
X-ray-induced HPRT$^-$ mutants		
HX101,[b] 216, 236, 312, 321, 324, 335, 338, 344, 349, 350,[c] 352, 353, 357, 359, 368	47, XY, +13, 14q+, 21p+	10/10
HX91	47, t(X;22)(q21.2;q13.2)Y, +13, 14q+, 21p+, **22p+**	9/10
	47, t(X;22)(q21.2;q13.2)Y, +13, 14q+, 21p+, **22p+**[d]	1/10
HX96	47, t(X;22)(q21.2;q13.2)Y, +13, 14q+, 21p+, **der(1), der(6)**	10/10
HX100	47, t(X;22)(q21.2;q13.2)Y, +13, 14q+, 21p+, **t(1;7)(q23;q33)**	6/6
HX235	47, XY, +13, 14q+, 21p+, 13s+	3/7
	46, XY, +13, 14q+, 21p+, 13s+, **−14**	1/7
	46, XY, +13, 14q+, 21p+, 13s+, **der(2)**, **−10**, **t(15;18)(q21;q23)**	1/7
	47, XY, +13, 14q+, 21p+, 13s+, **der(11)**	1/7
	47, XY, +13, 14q+, 21p+, 13s+, **20p+**	1/7
HX303	47, **t(X;11)(p21;q14)**Y, +13, 14q+, 21p+	10/10
HX304	47, XY, +13, 14q+, 21p+, 13s+, **t(3;13)(p21;q22)**, **der(5)**, **der(12)**, **−18**, **+mar**	10/10
HX309	47, XY, +13, 14q+, 21p+, **21q+**	6/10
	46, XY, +13, 14q+, 21p+, **−21**	1/10
	47, XY, +13, 14q+, 21p+, **+6**, **−21**, **del(5)(p11)**	1/10
	46, XY, +13, 14q+, 21p+, **10, t(10;21)(q11.2;q22.3)**	1/10
	46, XY, +13, 14q+, 21p+, **del(2)(q11.2)**, **−10**, **t(10q+;21q)**[e]	1/10
HX316	47, XY, +13, 14q+, 21p+, **t(8;15)(q13;q13)**	8/10
	47, **der X**, Y, +13, 14q+, 21p+, **t(8;15)(q13;q13)**, **del(16)(q11.2)**	1/10
	47, XY, +13, 14q+, 21p+, **t(8;15)(q13;q13)**, **del(4)(p12)**	1/10
HX329	47, **(Xq+)**Y, +13, 14q+, 21p+	9/10
	47, **(Xq+)**[f]Y, +13, 14q+, 21p+	1/10
γ-Irradiated clones		
IR1, 2, 3, 4, 5, 6, 7, 8, 9, 10, 11, 13, 14, 15, 16, 17, 18, 19, 22, 23, 25	47, XY, +13, 14q+, 21p+	10/10
IR12	47, XY, +13, 14q+, 21p+, **t(11;17)(p13;q22)**	10/10
IR20	48, XY, +13, 14q+, 21p+, **+20**	7/10
	47, XY, +13, 14q+, 21p+	2/10
	48, XY, +13, 14q+, 21p+, **t(14;19)(q23;p13.2)**, **+20**	1/10
IR21	47, XY, +13, 14q+, 21p+	9/10
	47, XY, +13, 14q+, 21p+, **del(13)(q22)**	1/10
IR24	47, XY, +13, 14q+, 21p+	5/10
	46, X, +13, 14q+, 21p+, **−Y**	3/10
	48, XY, +13, 14q+, 21p+, **+21**	2/10
Spontaneous HPRT$^-$ mutants		
HS20,[b] 266, 272, 274, 279[c]	47, XY, +13, 14q+, 21p+	20/20
HS33	47,t(X;22)(q21.2;q13.2)Y, 14q+, 21p+, **t(10;13)(q11.2;q14)**	20/20
HS34	47, X, +13, 14q+, 21p+, **+13**, **−Y**	20/20
HS622	48, XY, +13, 14q+, 21p+, **+20**	20/20
Untreated clones		
TK6-1, 2, 3, 6, 8, 9, 10	47, XY, +13, 14q+, 21p+	10/10
TK6-4	47, X**t(Y;9)(q11.23;p11)**, +13, 14q+, 21p+	10/10
TK6-5[g]	46, XY, 14q+, 21p+	10/10
TK6-7	48, XY, +13, 14q+, 21p+, **+20**	10/10

[a] Chromosomal aberrations defined as complex chromosomal rearrangements are underlined. Karyotypic abnormalities are shown in boldface type.
[b] The t(X;22)(q21.2;q13.2) seen in these mutants was found commonly in a subpopulation of TK6 cells from which these were derived.
[c] 13s+ appears to be a polymorphism within the TK6 population affecting the size of the satellite region on chromosome 13p. It is therefore not included in consideration of abnormalities.
[d] The smaller 22p addition appears to be derived by terminal deletion of the 22p+ in the majority karyotype.
[e] Appears to be derived from karyotype 4.
[f] The smaller Xq addition appears to be derived by terminal deletion of the Xq+ region in the majority karyotype.
[g] This mutant is missing the +13 seen in the normal TK6 karyotype.

RESULTS

Delayed chromosomal instability in irradiated TK6 cells. Clonal karyotypic analysis was performed using G-banding on four groups of clones derived from TK6 human lymphoblasts: 25 HPRT$^-$ mutants induced by exposure to 2 Gy of X rays; 8 spontaneous HPRT$^-$ mutants; 25 clones γ-irradiated with 2 Gy, not selected with 6-TG; and 10 unirradiated TK6 clones, not selected with 6-TG (Table 1). G-banding analysis was performed approximately 50 to 60 generations after seeding of cells for clonal isolation. The parental TK6 karyotype includes three characteristic abnormalities and is highly stable (Fig. 1A; Table 1). However, G-banding analysis (Table 1; Fig. 2A) demonstrated that both groups of irradiated clones are distinguished by karyotypic heterogeneity.

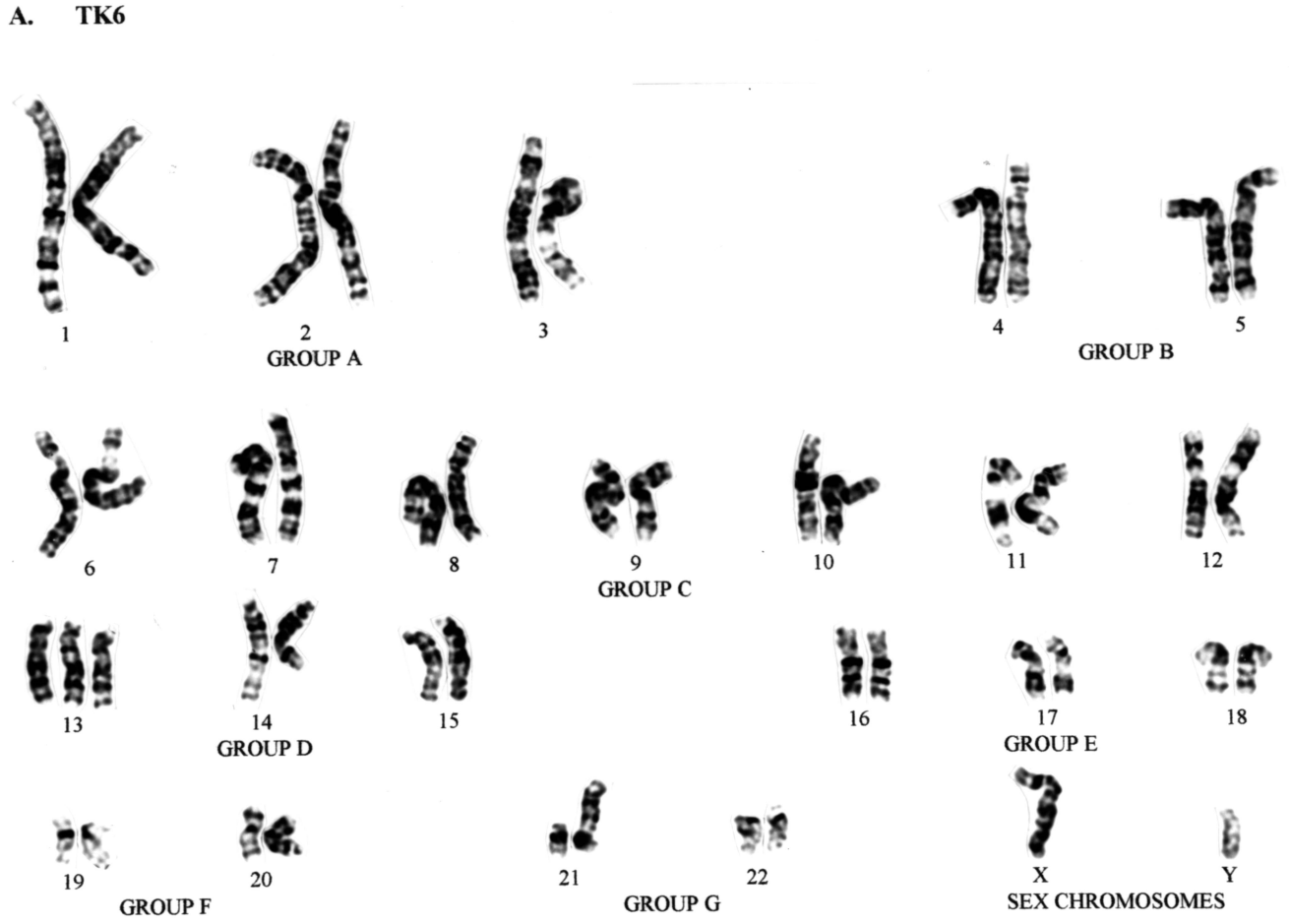

FIG. 1. (A) The parental TK6 karyotype. Three characteristic abnormalities (+13, 14q+, and 21p+) are found in all TK6 cells; furthermore, a t(X;22)(q21.2;q13.2) was found in a subpopulation of some TK6 cells (not shown). (B) Complex chromosomal rearrangement in HX91. (Left to right) 1, normal chromosome 22; 2, terminal addition (22p+) (a large, undefined terminal addition on the p arm of chromosome 22); 3, terminal deletion (22p+) (further modification of the rearranged chromosome observed in another metaphase by partial, terminal deletion of the 22p+ addition). (C) Complex chromosomal rearrangement in HX309. (Left to right) 1, normal chromosomes 10 and 21; 2 translocation [t(10;21)(q11.2;q22.3)] (a nonreciprocal translocation in which the q arm of chromosome 10 is added to the terminus of 21q; the junction region involves sequences at or near the chromosome 10 centromere); 3, terminal addition [t(10q+;21q)] (further modification of the rearranged chromosome observed in another metaphase by addition to the end of the translocated 10q; the banding pattern suggests that the added segment is derived from 10q).

Clones were classified as karyotypically heterogeneous if two or more distinct metaphases, exhibiting nonidentical chromosomal abnormalities, were observed; classification of a metaphase as distinct relied primarily on the occurrence of structural rearrangements. An occurrence of aneuploidy was used as a parameter of heterogeneity only in cases where it was observed in multiple metaphases; the gain or loss of a single chromosome in an individual metaphase was regarded as potentially artifactual and not counted in summary statistics. Distinct karyotypes are listed separately in Table 1 with karyotypic abnormalities shown in boldface type. Clonal karyotypic heterogeneity was common among irradiated clones, although the incidence of karyotypic heterogeneity in X-ray-induced $HPRT^-$ mutants was greater than observed in clones treated with radiation alone (Table 1; Fig. 2A). However, no karyotypic heterogeneity was observed in spontaneous $HPRT^-$ mutants or in untreated clones (Table 1; Fig. 2A).

The karyotypic instability of radiation-induced $HPRT^-$ mu-

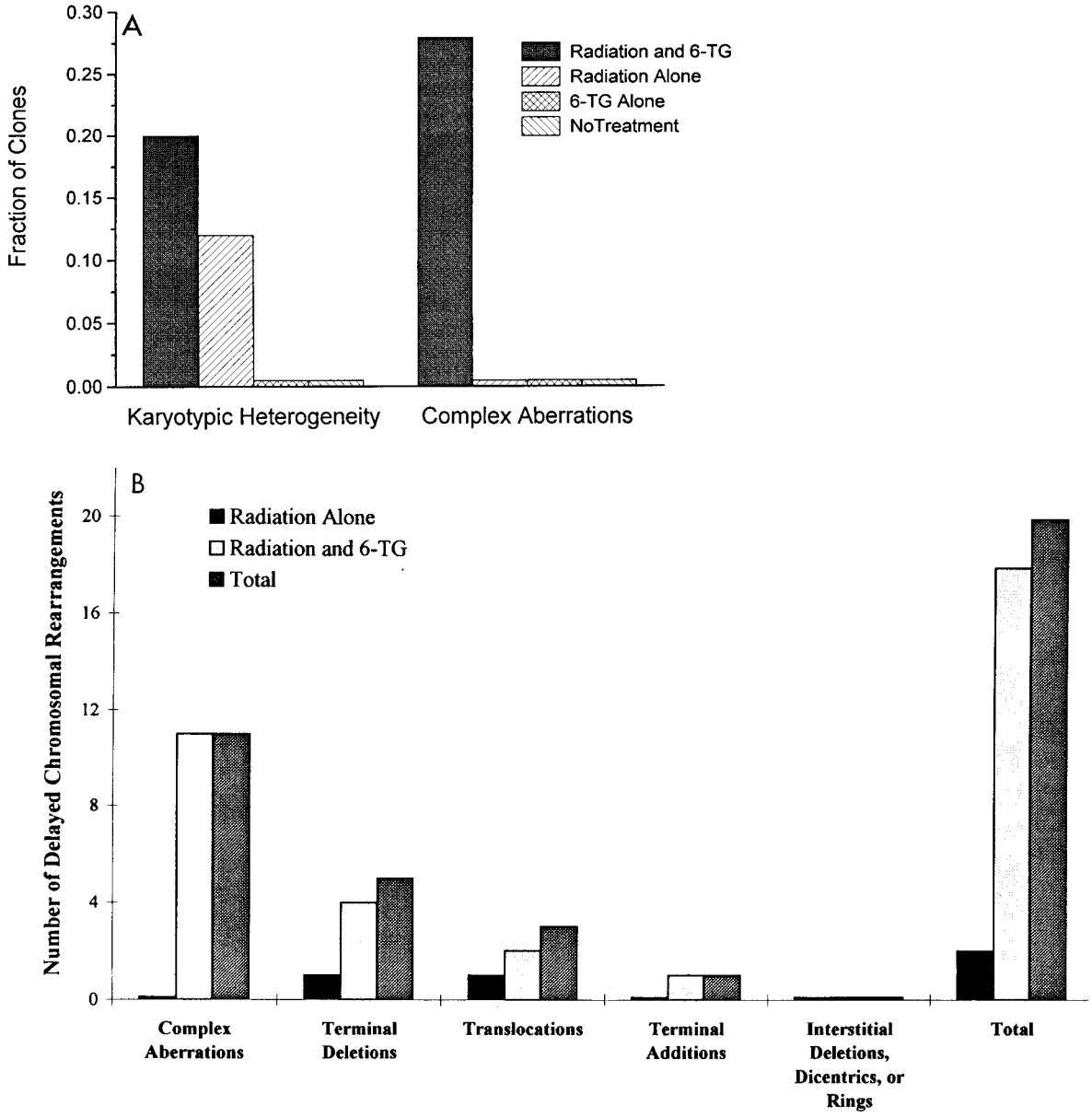

FIG. 2. (A) Frequency of delayed karyotypic instability among radiation-treated and control clones. Clonal karyotypic heterogeneity was defined as multiple, distinct metaphases in a single clone. Classification of a metaphase as distinct relied primarily on the occurrence of structural rearrangements, although aneuploidy was used as a parameter of heterogeneity in cases where it was observed in multiple metaphases. Complex aberrations included chromosomes containing two or more identifiable rearrangements, derivative chromosomes containing multiple rearrangements, and marker chromosomes which are extensively rearranged. (B) Categories of delayed chromosomal rearrangements identified in clonal analysis of irradiated cells. Individual chromosomal abnormalities were assigned to a unique category, although some complex aberrations involved identifiable terminal deletions or additions. (C) Translocations and terminal deletions preferentially involve breakage at or near the centromere. Centromeric breaks are defined by G-banding analysis to occur within the region of the centromere or pericentric heterochromatin. Breaks which are distal to the centromere occurred outside of the heterochromatic region. Both groups of rearrangements involved the deletion or translocation of the entire chromosome arm distal to the breakage site.

tants was also exhibited in other unique manifestations which were not observed in any of the other experimental groups. These manifestations include two clones (HX235 and HX309 [Table 1]) which exhibited four to five distinct metaphase karyotypes, many examples of metaphases with two or more independent chromosomal rearrangements (HX235, 304, 309, and 316 [Table 1]), and several examples of complex chromosomal aberrations (Table 1; Fig. 1B and C and 2A). In this investigation, complex aberrations were defined as containing two or more identifiable chromosomal rearrangements affecting a single chromosome, a derivative chromosome containing multiple rearrangements yet still cytogenetically recognizable, or a marker chromosome which is extensively rearranged and no longer cytogenetically distinguishable. Complex rearrangements involving two or more defined events on a single chromosome (HX91, 309, and 329) and derivative or marker chromosomes (HX96, 235, 304, and 316) were each observed in several radiation-induced 6-TG^R clones (Table 1; Fig. 1B and C and 2A). This extensive instability is unlikely to be attributable to the HPRT$^-$ phenotype, since no karyotypic heteroge-

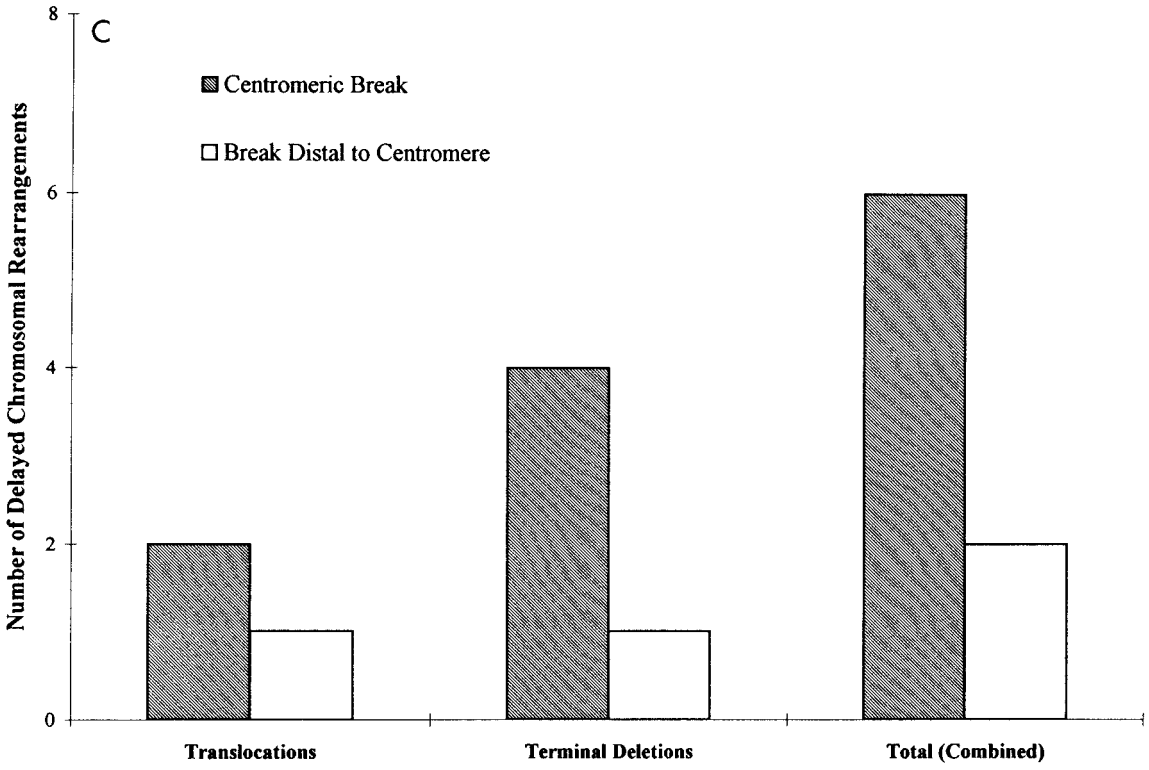

FIG. 2—*Continued.*

neity or complex chromosomal rearrangement was observed among spontaneous HPRT$^-$ mutants (Table 1; Fig. 2A). An alternate possibility is that exposure to 6-TG enhances karyotypic instability in surviving progeny of irradiated cells.

Delayed chromosomal aberrations preferentially occur near prior rearrangements and in centromeric regions. A total of 20 chromosomal aberrations occurring in irradiated clones were attributed to chromosomal instability since they were either nonclonal or scored as a complex aberration (Table 1; Fig. 2B). Among this group, 11 (0.55) were complex abnormalities. Delayed chromosomal rearrangements also included terminal deletions, additions, and translocations, although no example of an interstitial deletion was observed (Fig. 2B). These results suggest that delayed chromosomal aberrations frequently result following the generation of an acentric fragment which can then lead to a terminal deletion or addition, to a translocation, or to further development of a complex chromosomal rearrangement. For example, three definable terminal deletion or addition events were observed (HX91, 309, and 329 [Table 1; Fig. 1]) as a component of a complex chromosomal abnormality. For other complex rearrangements, scored as derivative or marker chromosomes, the breakage events could not be precisely defined. However, the prevalence of complex rearrangements indicates that delayed aberrations preferentially occur near the site of a previous chromosomal rearrangement. Furthermore, most of the noncomplex, delayed chromosomal rearrangements were attributable to a break near the centromere (six of eight [Fig. 2C]), resulting in deletion or translocation of the entire chromosome arm. These data suggest that centromeric and pericentric heterochromatic regions are also preferential targets for breakage associated with delayed chromosomal rearrangements. In addition to structural rearrangements, several examples of delayed aneuploidy occurring in more than one metaphase were found in irradiated clones (HX309, IR20, and IR24) but never in clones within the unirradiated experimental groups (Table 1).

A persistent mutator phenotype is associated with complex chromosomal rearrangements. In order to determine if karyotypically identified genetic instability affected specific locus mutation rates, we utilized the *tk* locus as a genetic marker. Four X-ray-induced HPRT$^-$ mutants with extensive karyotypic heterogeneity, and which exhibited the generation of complex chromosomal abnormalities during clonal outgrowth (HX235, 309, 316, and 329 [Table 1]), were examined. A statistically significant increase in the mutation rate of normal-growth TK$^-$ mutants was observed, ranging from four- to eightfold higher than that of the parental TK6 cells (Table 2). Mutation rates were determined for several additional controls, including three clones irradiated with 2 Gy of γ rays alone. Two of these clones (IR20 and 21 [Table 1]) exhibited clonal karyotypic heterogeneity but no complex chromosomal abnormalities, and no elevation of mutation rate was observed for this group (Table 2, group 2). Additionally, mutation rates were determined for three spontaneous 6-TG^R clones and one X-ray-induced 6-TG^R clone which did not exhibit clonal karyotypic heterogeneity or complex chromosomal abnormalities (Table 2, groups 3 and 4). A statistically significant elevation in mutation rate was observed between the mutants in group 1 compared with the overall mean mutation rate for groups 2 to 5 (Table 2) ($P = 0.0002$). A similar effect was observed for the mutation rate of slow-growth TK$^-$ mutants; even by using minimal estimates for clones exhibiting karyotypic instability, a highly significant increase of the slow-growth mutation rate was observed compared with that for control groups (Table 2) ($P = 0.007$). These mutation rates were determined approximately 80 to 100 cell generations after initial treatment with X-irradiation and selection in 6-TG. Therefore, these results indicate that a persistent mutator phenotype, as evidenced by

TABLE 2. Elevated TK$^-$ mutation rates in X-ray-induced HPRT$^-$ mutants exhibiting clonal karyotypic heterogeneity

Group and mutant	Mutation rate (10^{-7})	
	Normal growth	Slow growth
1. X-irradiated HPRT$^-$ clones exhibiting genetic instability		
HX235	>4.8	ND[a]
HX309	4.3	>6.7
HX316	7.5	>10.5
HX329	5	>9.8
Mean (group 1)	5.4[b]	9.0[c]
2. γ-irradiated clones		
IR14	2.1	6.4
IR20	1.6	5.5
IR21	0.85	3.7
3. Spontaneous HPRT$^-$ mutants		
HS34	2.8	ND
HS266	2.1	ND
HS504	0.98	3.3
4. X-irradiated HPRT$^-$ mutant not exhibiting genetic instability: HX216	2.8	5.1
5. Parental TK6 cells (nonclonal)	0.97	2.1
Mean (groups 2–5)	1.8[b]	4.4[c]

[a] ND, not determined.
[b] Significantly different as determined by a two-tailed, unpaired *t* test (P = 0.0002).
[c] Significantly different as determined by a two-tailed, unpaired *t* test (P = 0.007).

a significant increase in specific locus mutation rate, can be associated with extensive karyotypic instability.

Mutational specificity of the mutator phenotype. Mutants at the *tk* locus in TK6 lymphoblasts have been divided into normal-growth and slow-growth phenotypes (34, 39, 68). The slow-growth mutants have been shown to reflect extensive LOH on chromosome 17q and presumably involve a telomeric locus required for the normal cell growth rate (1, 7, 36, 67). In contrast, LOH occurring among normal-growth mutants generally involves an interstitial segment of chromosome 17q (1, 7, 36, 67). In studies in our laboratory (15a), microsatellite mapping of LOH tracts determined that only 1 of 28 normal-growth, but each of 26 slow-growth, TK$^-$ mutants encompassed the telomeric microsatellite marker D17S928. Categorization of individual TK$^-$ mutants, using growth rates and then molecular analysis of the normal-growth mutant cohort, was performed in order to investigate whether the mutations could be directly attributed to the delayed chromosomal rearrangements (Tables 3 and 4).

TABLE 3. Mutator phenotype in an altered mutational spectrum at the *tk* locus: LOH in normal-growth TK$^-$ mutants

Mutant category	No. (%) of mutants		
	Spontaneous	Mutator[a]	X ray induced (200 cGy)
LOH[b]	42 (47)	24 (23)	106 (58)
Heterozygous	47 (53)	80 (77)	78 (42)
Total	89	104	184

[a] Mutator mutants are TK$^-$ mutants collected from HPRT$^-$ mutants induced by 200 cGy of X rays and exhibiting karyotypic heterogeneity and elevated mutation rates at *tk*. Selection of TK$^-$ mutants was performed 60 to 100 generations following initial exposure to X rays.
[b] The representation of LOH among spontaneous mutants and mutator mutants is significantly different (P = 0.0005) as determined by Fisher's exact test. The representation of LOH among mutator mutants and X-ray-induced mutants is significantly different ($P < 0.0001$) as determined by Fisher's exact test.

TABLE 4. Mutator phenotypes in an altered mutational spectrum at the *tk* locus: mutation rates for LOH and intragenic mutations

Mutant category	Mutation rate (10^{-7})[a]		
	Spontaneous	Mutator	Induced
Overall	3.1	14.4	11.3
Normal growth (heterozygous)	0.51	4.2	3.7
Normal growth (LOH)	0.46	1.2	0.74
Slow growth (LOH)[b]	2.1	9.0	6.9

[a] Spontaneous mutation rates are derived from the value determined for TK6 cells (Table 2) and where appropriate are multiplied by the fraction of LOH or heterozygous mutants as previously determined (Table 3) (14). The data for the mutator clones have been similarly calculated. The induced mutation rate represents the value measured for the mutator clones with the background value for spontaneous clones subtracted out.
[b] Slow-growth mutants have been demonstrated previously to be almost entirely attributable to large-scale LOH of *tk*, extending through the end of 17q (1, 7, 15a, 36, 67).

For molecular analysis, 104 normal-growth TK$^-$ mutants were collected from the four mutator clones (Table 2, group 1). A statistically significant decrease in the representation of LOH mutants was observed among this collection of mutants compared with that among normal-growth TK$^-$ mutants arising spontaneously (P = 0.0005) (Table 3) or induced by γ radiation ($P < 0.0001$) (Table 3). The predicted relationship between delayed cytogenetic abnormalities and chromosomal-scale mutation was observed as a statistically significant increase in the mutation rate of slow-growth TK$^-$ mutants (P = 0.007) (Table 2), which corresponds with the prevalence of terminal deletions, additions, and translocations among delayed chromosomal abnormalities (Fig. 2B; Table 2). Mutation rates were estimated for each component of the spectrum (Table 4) by multiplying the mean mutation rates determined for the mutator clones (Table 2) by the fraction of LOH or heterozygous mutants (Table 3). A similar analysis of spontaneous mutation rates was derived from the value determined for TK6 cells (Table 2), multiplied by previously determined fractions of LOH and heterozygous mutants within the spontaneous spectrum (Table 3) (14). The induced mutation rate (Table 4) represents the value calculated for the mutator clones with the background value for spontaneous clones subtracted out. The induced mutation rate for slow-growth LOH mutants was nearly 10-fold higher than observed for normal-growth mutants exhibiting LOH (Table 4), which correlates with the absence of cytogenetically detectable interstitial deletions (Fig. 2B). Surprisingly, the mutator phenotype is also partially attributable to intragenic (heterozygous) TK$^-$ mutations (Tables 3 and 4).

DNA sequence analysis of TK$^-$ mutants derived from mutator clones. To determine if a specific point mutational type could be associated with the increased rate of intragenic TK$^-$ mutations, DNA sequencing and Southern analysis were performed on a representative set of 16 heterozygous TK$^-$ mutants. However, no predominant hot spot or specific mutational type was identified (Table 5). These data suggest that the mutator phenotype is mediated through a mechanism involved in a broad range of spontaneous mutations in parental TK6 cells. Structural rearrangements visible by Southern analysis accounted for 5 of 16 (31%) of the TK$^-$ mutants which remained heterozygous, which is comparable to previous reports of spontaneous normal-growth TK$^-$ mutants derived from TK6 cells (9 of 30, 30%) (16, 69). The TK$^-$ point mutants were

TABLE 5. DNA sequence analysis of TK^- mutants derived from mutator clones

Type and mutant	Position(s)[a]	Genomic alteration	Amino acid change or cDNA alteration	Target sequence[b]
Transitions				
M9	E3:164	AT→GC	Leu→Ser	AGAGT T GATGA
M2	E3:173	GC→AT	Arg→His	GAGAC G CGTCC
M13	E5:385	GC→AT	Glu→Lys	TCTGC G AGGCC
M12	E7:614	GC→AT	Arg→Gln	GTGTC G GCTCT
Transversions				
M20	E3:176	AT→TA	Val→Asp	ACGCG T CCGTC
M19	E3:260	AT→TA	His→Leu	CACAC A TGACC
M10	I5:11991	GC→TA	From use of cryptic splice donor at 12009, 18-bp insertion between exons 5 and 6	GGAAG g taaggcgtctgatccag(gt)ctgg
M1	E7:574	GC→TA	Glu→Stop	agGTC G AGGTG
Multiple substitution (M11)	E5:393, 403	GC→TA, GC→AT	Met→Ile, Gly→Arg	GCCAT G GCCAACGCC G GGAAG
Frameshift (M6)	E7:[607–611]	−GT	Deletion frameshift	ACTCC [GTGTGT] CGGCT
Deletions				
M8	E1:522–I2:2206	1,685-bp deletion	3′ region of exon 1, and all of exon 2, missing	GCCC[T]GGC . . . . ggatat[t]ataccc
M4	E6:12414–12428	15-bp deletion	In-frame deletion of 5 codons	TGTGCATGGAGTGCTTCCGGGAAGC
Structural rearrangements				
M3	Deletion involving exon 3		Exon 3 missing from cDNA	
M5	Deletion involving exon 3		Exon 3 missing from cDNA	
M16	Deletion involving exon 3		Not determined	
M17	Deletion involving exon 3		Not determined	

[a] Mutated positions are identified by the exon (E1 to E7) or intron (I1 to I6) in which they occur. Mutations occurring in exons are numbered according to their cDNA position. Mutations occurring in introns are numbered according to the genomic sequence position. Mutations are listed, within category, by order along the gene.

[b] The affected base or bases are indicated by spacing. Regions of ambiguity in frameshift mutants are indicated with brackets. Deleted sequences are indicated by underlining. A cryptic splice donor site used in mutant M10 is indicated with parentheses. Exon sequences are shown in uppercase, and intron sequences are shown in lowercase.

characterized by cDNA sequencing and additional genomic sequence analysis as required (Table 5). Single-base substitutions are evenly divided between transitions and transversions; one frameshift, two intragenic deletions, and one nontandem double-base substitution were also recovered. In all, 7 of the 10 base substitutions occurred at GC base pairs, including both of the changes in the nontandem double mutant (M11) (Table 5), closely reflecting the 60% GC content of the *tk* locus. However, each mutation at a GC base pair affected the G on the nontranscribed strand (Table 5), suggesting some possibility of strand bias.

DISCUSSION

Current models of carcinogenesis suggest that mutator phenotypes are crucial in the accumulation of multiple mutations required for the emergence of a malignant tumor (8, 33, 40, 49). In this study the specificity of delayed chromosomal rearrangements, and the corresponding generation of mutations at the autosomal marker locus *tk*, was examined.

Genomic instability induced by sparsely ionizing radiation can be enhanced by other factors. Recent reports have shown that delayed chromosomal instability is consistently induced by densely ionizing radiation but only occasionally observed in cultures exposed to X-irradiation. Chromosomal instability was demonstrated in mouse (27) and human (25, 26) hemopoietic stem cells and in primary human fibroblasts (42, 56) following exposure to high-energy particles, but instability was not observed when parallel experiments were conducted using X rays (25–27). However, X-ray-induced delayed chromosomal instability has been reported in a human-hamster hybrid cell line which is deficient in p53 activity (41) and in human T-lymphocyte clones (20, 21) which were stimulated for growth in vitro with phytohemagglutinin. In this investigation, clonal karyotypic heterogeneity was observed among clones exposed to X-irradiation alone, and comparable levels were observed among X-ray-induced $HPRT^-$ mutants (Table 1; Fig. 2). However, several additional parameters indicate that chromosomal instability was more extensive in the irradiated $6\text{-}TG^R$ clones. In particular, complex rearrangements were commonly observed among clones exposed to both X-rays and 6-TG (7 of 25, 28%) but were not found in any of the other experimental groups (0 of 43, $P = 0.0005$) (Table 1; Fig. 2). $HPRT^-$ spontaneous mutants did not exhibit any parameter of genetic instability and had aberration frequencies similar to that of untreated control cells, suggesting that 6-TG by itself causes little or no chromosomal instability but can enhance the delayed effects of radiation exposure. Taken as a whole, the results of this investigation (Fig. 2; Table 1) and previous studies (25–27) indicate that the induction of genetic instability by sparsely ionizing radiation may be significantly enhanced by cellular apoptosis deficiency (41), by agents which stall DNA replication such as 6-TG (see below), and potentially by treatment with mitogens such as phytohemagglutinin (20, 21).

One possibility for the effect of 6-TG is that selecting for mutant cells also enhanced the representation of genetically unstable cells in the population. This possibility seems unlikely since in preliminary experiments (15b) examining radiation-induced TK^- mutants, chromosomal instability resembled clones receiving radiation alone rather than radiation-induced $HPRT^-$ mutants (Table 1). In particular, no complex chromosomal abnormalities were identified, although clonal karyo-

typic heterogeneity was observed. This provides evidence against the hypothesis that selection of mutants enriches the population for genetic instability and suggests instead a specific 6-TG effect. We suggest that the effect of 6-TG is attributable to abnormal DNA replication, since exposure to 6-TG has been shown to result in stalling of the replication fork, even in cell lines which are HPRT deficient (17, 22, 46). Chromosomal breakage occurring at stalled replication bubbles has been previously proposed as an initial step in the occurrence of gene amplification and generalized chromosomal instability (65, 66). The synergistic interaction between X-irradiation and 6-TG was observed despite a 7-day phenotypic expression interval between exposure to the two agents, suggesting that irradiated cells contain chromosomal regions which are persistently hypersensitive to the effects of 6-TG. The mechanism for such hypersensitivity remains unknown, but possibilities include regional modification of higher-order chromatin structure or abnormal relationship to the nuclear matrix. Such alterations may be prevalent in regions near a previous chromosomal rearrangement junction (55, 64). Indeed, our results (Table 1) and previous studies (20, 21, 41) demonstrate that a large majority of delayed chromosomal aberrations occur near the position of a previous rearrangement.

Specificity of delayed chromosomal aberrations. In this investigation, the observation of clonal karyotypic heterogeneity, particularly evidence of sequential events affecting specific chromosomes, indicated that chromosomal rearrangements occurred many generations after radiation exposure. The use of G banding permits the chromosomal specificity of these delayed rearrangements to be examined. The data presented here and in other studies (20, 21) provide no evidence for the preferential involvement of specific chromosomes in delayed rearrangements. However, sequential rearrangements leading to a progressively abnormal chromosome have been reported to be frequent events in radiation-induced instability (41), and the observation of complex rearrangements in clonal analysis may reflect this sequential process (29). Instances of trisomy 20 were seen in three clones (IR20, HS622, and TK6-7 [Table 1]), and this may reflect a selective advantage for this karyotypic modification in TK6 cells. However, no clone was classified as heterogeneous on the basis of only this parameter, and only one karyotypically heterogeneous clone (IR20) exhibited trisomy 20. Therefore, there appears to be no evidence that clonal karyotypic heterogeneity is attributable to selective pressures rather than induced instability, since the same structural rearrangement was never observed to reoccur in independent clones.

A total of 20 chromosomal aberrations were attributed to delayed chromosomal instability, and among this group 11 (0.55) were complex aberrations (Fig. 2B). A similar prevalence (18 of 33, 0.55) was reported for the occurrence of independent marker chromosomes among delayed chromosomal aberrations in X-irradiated T lymphocytes also analyzed by G banding (20). These data indicate that delayed aberrations preferentially occur near the site of a previous chromosomal rearrangement. Complex chromosomal abnormalities were observed only in the experimental group exposed to radiation and 6-TG (Table 1; Fig. 1) and appear to be characteristic of a relatively high rate of persistent genetic instability which correlates with the occurrence of delayed TK^- mutations. However, even in clones with elevated mutation rates, unstable abnormalities such as rings, dicentrics, and chromatid type aberrations were not observed among the delayed chromosomal rearrangements (Table 1; Fig. 2B). This suggests that the rate of chromosomal instability is lower than the rate of instability induced by high-LET radiation (25–27, 42) or instability in p53-deficient cell lines (41). Kadhim et al. (26) also observed that compared with α-particles, X rays induce a different pattern of delayed rearrangements which was predominated by chromosome type aberrations.

The noncomplex, delayed chromosomal rearrangements most often resulted from a break at or near the centromere (Fig. 2C), which generated a deletion or translocation of the entire chromosome arm (Fig. 2B). Terminal deletion or addition events were also observed as a component of complex chromosomal abnormalities (Table 1; Fig. 1). No case of an interstitial chromosomal deletion as a delayed event was observed. Furthermore, the absence of delayed interstitial deletions does not reflect a biological or methodological restriction, since they are commonly recovered in TK6 cells as clonal events at early times after X-irradiation (15c, 30).

Chromosomal instability appears to be closely related to the mechanisms of gene amplification, and specific models have been proposed to account for collateral chromosomal alterations in addition to amplification of target gene sequences (58, 62, 63, 65, 66). Previous reports have indicated that the formation of dicentric chromosomes which participate in bridge-breakage-fusion cycles (43, 44, 62, 63) may explain the repeated rearrangement of individual chromosomes in chromosomal instability and the amplification of target genes in a directly related process. This model predicts that terminal translocations and deletions would occur randomly along the chromosome because of mechanical shearing as the two centromeres are pulled to opposite poles during anaphase. However, breakage leading to delayed translocations and deletions in TK6 cells preferentially occurred near the centromere (Table 1; Fig. 2C).

An alternative model (65, 66) invokes chromosomal breakage at a stalled replication bubble and uneven segregation of replication-competent acentric fragments as the initial event in amplification. Evidence for chromosomal instability and chromosomal-scale mutations, following the generation of an acentric fragment broken within subcentromeric heterochromatin, has been previously reported (59). The data presented here suggest that radiation-induced delayed chromosomal rearrangements could arise through a similar mechanism involving the generation of an acentric fragment following breakage at centromeric or pericentric heterochromatic regions. The acentric fragment can then become deleted or translocated and thus frequently result in the juxtaposition of euchromatin with centromeric heterochromatin. Analysis of complex chromosomal rearrangements demonstrates that they too can result from sequential terminal deletion and addition events. Therefore, we suggest that the predominance of delayed abnormalities near previous rearrangements indicates that regions surrounding rearrangement junctions involving centromeric heterochromatin are particularly susceptible to further breakage.

Delayed TK^- mutations in clones exhibiting genomic instability. Previous investigations have found that genetic instability, occurring in tumors or malignantly transformed cell lines (2, 3, 9, 10, 13, 24, 57, 61), is inconsistently associated with elevated rates of mutation. However, these studies have been largely restricted to the use of marker genes which are insensitive to chromosomal mechanisms of mutagenesis. The predicted relationship between cytogenetic instability and chromosomal scale mutations was demonstrated by using the heterozygous, autosomal marker locus *tk*. The rate of intragenic TK^- mutations was unexpectedly also significantly increased 70 to 80 generations after irradiation and clonal selection (Table 4). These intragenic mutations may be related to a report of increased mutation frequency at the hemizygous *hprt*

locus in clonal populations of CHO cells examined up to 100 generations after X-irradiation (6). DNA sequence analysis was performed for some of the intragenic TK^- mutants (Table 5) but provided no evidence for a specific hot spot or class of mutation to account for the additional increment of mutations. Elevated rates of chromosomal-scale and intragenic mutations may be attributable to independent processes, but their coincident appearance in the same clones indicates that they may each be a manifestation of a single underlying mechanism. Mismatch repair has received a great deal of recent attention due to the associated microsatellite instability and increased point mutation rates observed in cells from patients with hereditary nonpolyposis colon cancer (3, 10). However, hereditary nonpolyposis colon cancer cells exhibit no chromosomal instability (3, 10, 45, 54), and thus, mismatch repair deficiency is unlikely to provide a full explanation for the results presented here.

Complex chromosomal abnormalities appear to be the best cytogenetic indicator of clones with elevated mutation rates (Tables 1 and 2). Clones which exhibited karyotypic heterogeneity in the absence of complex abnormalities did not demonstrate an increase in the rate of either intragenic or chromosomal-scale mutations (Tables 1 and 2). Complex chromosomal abnormalities may be a good indicator of elevated rates of delayed mutation, since clones which exhibit complex rearrangements have far more individual structural alterations than those clones which exhibit karyotypic heterogeneity only (Table 1). Many of the complex chromosomal abnormalities have a large but undetermined number of rearrangements on single chromosomes which are listed once only as derivatives or markers (Table 1). This provides evidence that the rate of chromosomal instability is much higher in clones containing a complex rearrangement, and therefore, it is unsurprising that the delayed mutation rates reflect the higher rate of delayed chromosomal abnormalities. Clones which exhibit only karyotypic heterogeneity may also have a slight increase in specific locus mutation rate, reflecting the relatively low rate of delayed chromosomal rearrangements; any such increase was not detected as a statistically significant increase in the TK^- mutation rate (Table 2).

The relationship between delayed mutations and delayed chromosomal rearrangements was suggested by mutational spectrum analysis (Tables 2 to 4). Normal-growth TK^- mutants arise because of intragenic or interstitial chromosomal events, while slow-growth TK^- mutants uniformly undergo LOH encompassing telomeric polymorphic genetic markers (1, 7, 15a, 36, 67). Therefore, the recovery of only slow-growth LOH mutants as delayed events (Tables 2 and 4) directly corresponds with the absence of interstitial deletions and the predominance of terminal deletions and translocations among delayed chromosomal rearrangements (Fig. 2B).

Conclusions. Delayed chromosomal rearrangements are most frequently complex abnormalities which are generated by repeated breakage of previously rearranged chromosomes. Noncomplex delayed rearrangements often follow breakage at centromeric or pericentric heterochromatic regions resulting in deletion or translocation of the entire acentric chromosomal arm. No example of a delayed interstitial deletion was observed. The specific recovery of slow-growth, chromosomal-scale, TK^- mutants provides support for conclusions regarding the specificity of delayed chromosomal rearrangements. The frequency of breakage at centromeric heterochromatin in noncomplex rearrangements, and the overall predominance of delayed abnormalities near sites of previous rearrangements, may indicate an important role for the juxtaposition of euchromatin with centromeric heterochromatin in the generation of delayed complex abnormalities.

ACKNOWLEDGMENTS

This work was supported by a grant to A.J.G. (RO1-CA55659) from the National Institutes of Health.

We thank David Wu for assistance with these experiments.

REFERENCES

1. **Amundson, S. A., and H. L. Liber.** 1992. A comparison of induced mutation at homologous alleles of the *tk* locus in human cells. II. Molecular analysis of mutants. Mutat. Res. **267:**89–95.
2. **Bailly, M., S. Bertrand, and J. F. Dore.** 1993. Increased spontaneous mutation rates and prevalence of karyotype abnormalities in highly metastatic human melanoma cell lines. Melanoma Res. **3:**51–61.
3. **Bhattacharyya, N. P., A. Skandalis, A. Ganesh, J. Groden, and M. Meuth.** 1994. Mutator phenotypes in human colorectal carcinoma cell lines. Proc. Natl. Acad. Sci. USA **91:**6319–6323.
4. **Cavenee, W. K., T. P. Dryja, R. A. Phillips, W. F. Benedict, R. Godbout, B. L. Gallie, A. L. Murphree, L. C. Strong, and R. L. White.** 1983. Expression of recessive alleles by chromosomal mechanisms in retinoblastoma. Nature (London) **305:**779–784.
5. **Chang, W. P., and J. B. Little.** 1991. Delayed reproductive death in X-irradiated Chinese hamster ovary cells. Int. J. Radiat. Biol. **60:**483–496.
6. **Chang, W. P., and J. B. Little.** 1992. Persistently elevated frequency of spontaneous mutations in progeny of CHO clones surviving X-irradiation: association with delayed reproductive death phenotype. Mutat. Res. **270:** 191–199.
7. **Chaudhry, M. A., Q. Jiang, M. Ricanati, M. F. Horng, and H. H. Evans.** 1996. Characterization of multilocus lesions in human cells exposed to x radiation and radon. Radiat. Res. **145:**31–38.
8. **Christians, F. C., T. G. Newcomb, and L. A. Loeb.** 1995. Potential sources of multiple mutations in human cancers. Prev. Med. **24:**329–332.
9. **Elmore, E., T. Kakunaga, and J. C. Barrett.** 1983. Comparison of spontaneous mutation rates of normal and chemically transformed human skin fibroblasts. Cancer Res. **43:**1650–1655.
10. **Eshleman, J. R., E. Z. Lang, G. K. Bowerfind, R. Parsons, B. Vogelstein, J. K. Willson, M. L. Veigl, W. D. Sedwick, and S. D. Markowitz.** 1995. Increased mutation rate at the *hprt* locus accompanies microsatellite instability in colon cancer. Oncogene **10:**33–37.
11. **Fain, P. R., E. Solomon, and D. H. Ledbetter.** 1991. Second international workshop on human chromosome 17. Cytogenet. Cell Genet. **57:**66–77.
12. **Flemington, E., H. D. Bradshaw, V. Traina-Dorge, V. Slagel, and P. L. Deininger.** 1987. Sequence, structure and promoter characterization of the human thymidine kinase gene. Gene **52:**267–277.
13. **Frost, P., W. Kendal, B. Hunt, and M. Ellis.** 1988. The prevalence of ouabain-resistant variants after mutagen treatment. Lack of correlation between the frequency of variant expression and the metastatic phenotype. Invasion Metastasis **8:**73–86.
14. **Giver, C. R., S. L. Nelson, M. Y. Cha, P. Pongsaensook, and A. J. Grosovsky.** 1995. Mutational spectra of spontaneous and X-ray induced TK^- human cell mutants. Carcinogenesis **16:**267–275.
15. **Giver, C. R., S. L. Nelson, and A. J. Grosovsky.** 1993. Spectrum of spontaneous mutations in the human *hprt* gene. Environ. Mol. Mutagen. **22:**138–146.

15a. **Giver, C. R., K. K. Parks, and A. J. Grosovsky.** Unpublished observations.
15b. **Grosovsky, A. J., and K. K. Parks.** Unpublished observations.
15c. **Grosovsky, A. J., K. K. Parks, and S. L. Nelson.** Unpublished observations.

16. **Grosovsky, A. J., B. N. Walter, and C. R. Giver.** 1993. DNA-sequence specificity of mutations at the human thymidine kinase locus. Mutat. Res. **289:**231–243.
17. **Gusella, J. F., and D. Houseman.** 1976. Induction of erythroid differentiation *in vitro* by purines and purine analogs. Cell **8:**263–269.
18. **Harwood, J., and M. Meuth.** 1995. Deletion mapping of highly conserved transcribed sequence downstream from *aprt* locus. Somat. Cell Mol. Genet. **21:**151–160.
19. **Harwood, J., T. Tachibana, R. Davis, N. P. Bhattacharyya, and M. Meuth.** 1993. High rate of multilocus deletion in a human tumor cell line. Hum. Mol. Genet. **2:**165–171.
20. **Holmberg, K., S. Falt, A. Johannson, and B. Lambert.** 1993. Clonal chromosomal aberrations and genomic instability in X-irradiated human T-lymphocyte cultures. Mutat. Res. **286:**321–330.
21. **Holmberg, K., A. E. Meijer, G. Auer, and B. Lambert.** 1995. Delayed chromosomal instability in human T-lymphocyte clones exposed to ionizing radiation. Int. J. Radiat. Biol. **68:**245–255.
22. **Ishiguro, K., E. L. Schwartz, and A. C. Sartorelli.** 1984. Characterization of the metabolic forms of 6-thioguanine responsible for cytotoxicity and induction of differentiation of HL-60 acute promyelocytic leukemia cells. J. Cell. Physiol. **121:**383–390.
23. **Jaffe, D. R., J. F. Williamson, and G. T. Bowden.** 1987. Ionizing radiation

enhances malignant progression of mouse skin tumors. Carcinogenesis **8:**1753–1755.
24. **Kaden, D., I. K. Gadi, L. Bardwell, R. Gelman, and R. Sager.** 1989. Spontaneous mutation rates of tumorigenic and nontumorigenic Chinese hamster embryo fibroblast cell lines. Cancer Res. **49:**3374–3379.
25. **Kadhim, M. A., S. A. Lorimore, M. D. Hepburn, D. T. Goodhead, V. J. Buckle, and E. G. Wright.** 1994. Alpha-particle-induced chromosomal instability in human bone marrow cells. Lancet **344:**987–988.
26. **Kadhim, M. A., S. A. Lorimore, K. M. Townsend, D. T. Goodhead, V. J. Buckle, and E. G. Wright.** 1995. Radiation-induced genomic instability: delayed cytogenetic aberrations and apoptosis in primary human bone marrow cells. Int. J. Radiat. Biol. **67:**287–293.
27. **Kadhim, M. A., D. A. Macdonald, D. T. Goodhead, S. A. Lorimore, S. J. Marsden, and E. G. Wright.** 1992. Transmission of chromosomal instability after plutonium alpha-particle irradiation. Nature (London) **355:**738–740.
28. **Kallioniemi, A., O. P. Kallioniemi, D. Sudar, D. Rutovitz, J. W. Gray, F. Waldman, and D. Pinkel.** 1992. Comparative genomic hybridization for molecular cytogenetic analysis of solid tumors. Science **258:**818–821.
29. **Kano, Y., and J. B. Little.** 1985. Mechanisms of human cell neoplastic transformation: relationship of specific abnormal clone formation to prolonged lifespan in X-irradiated human diploid fibroblasts. Int. J. Cancer **36:**407–413.
30. **Kano, Y., and J. B. Little.** 1986. Site-specific chromosomal rearrangements induced in human diploid cells by x-irradiation. Cytogenet. Cell Genet. **41:**22–29.
31. **Kennedy, A. R.** 1991. Is there a critical target gene for the first step in carcinogenesis? Environ. Health Perspect. **93:**199–203.
32. **Kennedy, A. R., J. Cairns, and J. B. Little.** 1984. Timing of the steps in transformation of C3H 10T 1/2 cells by X-irradiation. Nature (London) **307:**85–86.
33. **Kronenberg, A.** 1994. Radiation-induced genomic instability. Int. J. Radiat. Biol. **66:**603–609.
34. **Kronenberg, A., and J. B. Little.** 1989. Molecular characterization of thymidine kinase mutants of human cells induced by densely ionizing radiation. Mutat. Res. **211:**215–224.
35. **Lasko, D., W. Cavenee, and M. Nordenskjold.** 1991. Loss of constitutional heterozygosity in human cancer. Annu. Rev. Genet. **25:**281–314.
36. **Li, C. Y., D. W. Yandell, and J. B. Little.** 1992. Molecular mechanisms of spontaneous and induced loss of heterozygosity in human cells *in vitro*. Somat. Cell Mol. Genet. **18:**77–87.
37. **Li, I. C., S. C. Wu, J. Fu, and E. H. Chu.** 1985. A deterministic approach for the estimation of mutation rates in cultured mammalian cells. Mutat. Res. **149:**127–132.
38. **Liber, H. L., and W. G. Thilly.** 1982. Mutation assay at the thymidine kinase locus in diploid human lymphoblasts. Mutat. Res. **94:**467–485.
39. **Liber, H. L., D. W. Yandell, and J. B. Little.** 1989. A comparison of mutation induction at the *tk* and *hprt* loci in human lymphoblastoid cells; quantitative differences are due to an additional class of mutations at the autosomal *tk* locus. Mutat. Res. **216:**9–17.
40. **Loeb, L. A.** 1991. Mutator phenotype may be required for multistage carcinogenesis. Cancer Res. **51:**3075–3079.
41. **Marder, B. A., and W. F. Morgan.** 1993. Delayed chromosomal instability induced by DNA damage. Mol. Cell. Biol. **13:**6667–6677.
42. **Martins, M. B., L. Sabatier, M. Ricoul, A. Pinton, and B. Dutrillaux.** 1993. Specific chromosome instability induced by heavy ions: a step towards transformation of human fibroblasts? Mutat. Res. **285:**229–237.
43. **McClintock, B.** 1941. The stability of broken ends of chromosomes in *Zea mays*. Genetics **26:**234–282.
44. **McClintock, B.** 1984. The significance of responses of the genome to challenge. Science **226:**792–801.
45. **Modrich, P.** 1994. Mismatch repair, genetic stability, and cancer. Science **266:**1959–1960.
46. **Morgan, C. J., R. N. Chawdry, A. R. Smith, G. Siravo-Sagraves, and R. W. Trewyn.** 1994. 6-thioguanine-induced growth arrest in 6-mercaptopurine-resistant human leukemia cells. Cancer Res. **54:**5387–5393.
47. **Mulcahy, R. T., M. N. Gould, and K. H. Clifton.** 1984. Radiogenic initiation of thyroid cancer: a common cellular event. Int. J. Radiat. Biol. Relat. Stud. Phys. Chem. Med. **45:**419–426.
48. **Muller, H., and R. Scott.** 1992. Hereditary conditions in which the loss of heterozygosity may be important. Mutat. Res. **284:**15–24.
49. **Murnane, J. P.** 1996. Role of induced genetic instability in the mutagenic effects of chemicals and radiation. Mutat. Res. **367:**11–23.
50. **Nelson, S. L., C. R. Giver, and A. J. Grosovsky.** 1994. Spectrum of X-ray-induced mutations in the human *hprt* gene. Carcinogenesis **15:**495–502.
51. **Nelson, S. L., I. M. Jones, J. C. Fuscoe, K. Burkhart-Schultz, and A. J. Grosovsky.** 1995. Mapping the endpoints of large deletions affecting the hprt locus in human peripheral blood cells and cell lines. Radiat. Res. **141:**2–10.
52. **Nelson, S. L., K. K. Parks, and A. J. Grosovsky.** 1996. Ionizing radiation signature mutations in human cell mutants induced by low dose exposures. Mutagenesis **11:**275–279.
53. **Nowell, P. C.** 1976. The clonal evolution of tumor cell progression for multistage carcinogenesis. Science **194:**23–28.
54. **Parsons, R., G. M. Li, M. J. Longley, W. H. Fang, N. Papadopoulos, J. Jen, A. de la Chapelle, K. W. Kinzler, B. Vogelstein, and P. Modrich.** 1993. Hypermutability and mismatch repair deficiency in RER^+ tumor cells. Cell **75:**1227–1236.
55. **Qumsiyeh, M. B.** 1995. Impact of rearrangements on function and position of chromosomes in the interphase nucleus and on human genetic disorders. Chromosome Res. **3:**455–465.
56. **Sabatier, L., B. Dutrillaux, and M. B. Martin.** 1992. Chromosomal instability. Nature (London) **357:**548.
57. **Seshadri, R., R. J. Kutlaca, K. Trainor, C. Matthews, and A. A. Morley.** 1987. Mutation rate of normal and malignant human lymphocytes. Cancer Res. **47:**407–409.
58. **Smith, K. A., P. A. Gorman, M. B. Stark, R. P. Groves, and G. R. Stark.** 1990. Distinctive chromosomal structures are formed very early in the amplification of CAD genes in Syrian hamster cells. Cell **63:**1219–1227.
59. **Smith, L. E., and A. J. Grosovsky.** 1993. Genetic instability on chromosome 16 in a human B lymphoblastoid cell line. Somat. Cell Mol. Genet. **19:**515–527.
60. **Solomon, E., J. Borrow, and A. D. Goddard.** 1990. Chromosome aberrations and cancer. Science **254:**1153–1160.
61. **Tagger, A. Y., J. E. Damen, A. H. Greenberg, and J. A. Wright.** 1989. Lack of correlation between deoxyribonucleotide pool sizes, spontaneous mutation rates and malignant potential in Chinese hamster ovary cells. J. Cancer Res. Clin. Oncol. **115:**429–434.
62. **Toledo, F., D. L. Roscouet, G. Buttin, and M. Debatisse.** 1992. Co-amplified markers alternate in megabase long chromosomal inverted repeats and cluster independently in interphase nuclei at early steps of mammalian gene amplification. EMBO J. **11:**2665–2673.
63. **Trask, B. J., and J. L. Hamlin.** 1989. Early dihydrofolate reductase gene amplification events in CHO cells usually occur on the same chromosome arm as the original locus. Genes Dev. **3:**1913–1925.
64. **Wallrath, L. L., and S. C. Elgin.** 1995. Position effect variegation in Drosophila is associated with an altered chromatin structure. Genes Dev. **9:**1263–1277.
65. **Windle, B., B. W. Draper, Y. Yin, S. O'Gorman, and G. M. Wahl.** 1991. A central role for chromosome breakage in gene amplification, deletion formation, and amplicon integration. Genes Dev. **5:**160–174.
66. **Windle, B. E., and G. M. Wahl.** 1992. Molecular dissection of mammalian gene amplification: new mechanistic insights revealed by analyses of very early events. Mutat. Res. **276:**199–224.
67. **Xia, F., S. A. Amundson, J. C. Nickoloff, and H. L. Liber.** 1995. Different capacities for recombination in closely related human lymphoblastoid cell lines with different mutational responses to X-irradiation. Mol. Cell. Biol. **14:**5850–5857.
68. **Yandell, D. W., T. P. Dryja, and J. B. Little.** 1986. Somatic mutations at a heterozygous autosomal locus in human cells occur more frequently by allele loss than by intragenic structural alterations. Somat. Cell Mol. Genet. **12:**255–268.
69. **Yandell, D. W., T. P. Dryja, and J. B. Little.** 1990. Molecular genetic analysis of recessive mutations at a heterozygous autosomal locus in human cells. Mutat. Res. **229:**89–102.